Infrared spectrum of the electron bubble in liquid helium

C. C. Grimes and G. Adams
AT&T Bell Laboratories, Murray Hill, New Jersey 07974
(Received 16 October 1989)

The energy of the ground-state–to–first-excited-state electronic transition in the electron bubble in liquid helium has been measured at 1.3 K and found to be 0.122 eV at a pressure of 1.1 atm and increasing to 0.209 eV at 18.3 atm. The spherical-square-well model of the electron bubble accounts well for the transition energies if the effective surface tension is taken to be independent of pressure. This model also yields improved values for the electron bubble radius as a function of pressure. The position of a line in the P-T plane where the photoconductivity signal vanishes indicates that trapping of electron bubbles on vorticity plays a role in the detection mechanism.

INTRODUCTION

It is well established that an excess electron in liquid helium resides in a cavity or bubble of radius ≈ 17 Å at zero pressure.[1] The electron bubble state occurs because the Pauli principle repulsion between an electron and helium atoms is strong, while the attractive polarization interaction is weak. The electron bubble that results is very nearly a textbook example of an electron confined in a spherical-square-well potential about 1 eV deep.

Spectroscopic studies on the electron bubble were first reported in 1967 when Northby and Sanders observed electronic transitions from the ground state to the continuum at a wavelength near 1.0 μm.[2] Their photoconductivity measurement was extended by Zipfel *et al.* to finite pressures and longer wavelengths (2.5 μm) where transitions to a bound state were observed and tentatively interpreted as the $1s$-$1p$ transition.[3,4] Later calculations by Miyakawa and Dexter (MD) indicated that the observed bound-state transition was probably the $1s$-$2p$ transition and that the $1s$-$1p$ transition, which has 97% of the oscillator strength, should occur at still longer wavelengths (near 11 μm).[5]

In this article we report the first measurements of the energy of the $1s$-$1p$ transition and its dependence on pressure for pressures to 18 atm. Our results thus confirm the interpretation of MD that Zipfel had observed the $1s$-$2p$ transition. Now, with more complete spectroscopy data available, we can use the spherical-square-well model to examine whether the well depth V_0 and the surface tension σ vary with pressure as expected from simple considerations. We find that our data and those of Zipfel agree well with the spherical-square-well model if $V_0(P)$ has the expected pressure dependence while σ is taken to be independent of pressure instead of having the expected rapid increase.

We have employed a simpler photoconductivity technique than was used by the earlier workers. We find evidence, as they did, that trapping of the electron bubbles on vorticity in the superfluid helium plays a role in the photoconductivity detection mechanism. However, as discussed below, we do not feel that simple photoejection out of "traps" on vorticity can account for our observations.

APPARATUS AND PROCEDURES

The source of infrared radiation for the experiment consists of a Nernst glower operating at 1750 K, a light chopper, and a diffraction grating monochromator having f-5 optics. The radiation from the monochrometer is focused into a 0.95 cm i.d. polished brass light pipe which guides the radiation to the experimental cell which is immersed in a pumped helium bath. Zinc selenide windows are mounted near the ends of the light pipe to permit its evacuation. The incident radiation is concentrated by a polished brass cone and enters the top of the experimental cell through a 0.6 cm i.d. or smaller opening. Two experimental cells have been used. The simplest is a circular cylinder 0.625 cm in diameter and 0.625 cm high containing near its center a single electrolytically sharpened tungsten field emission tip which serves as a source of electrons. The other cell is a 1.56 cm radius hemisphere containing five field emission tips, and has a mercury cadmium telluride (HgCdTe) photoconductive infrared detector coupled to the cell through a 0.3 cm diameter opening. This cell yielded useful photoconductivity data, and was also used, unsuccessfully, to search for transitions in direct infrared absorption. The interior surfaces of both cells are goldplated polished brass. The cell is contained inside a cylindrical vessel that is designed to withstand pressures to 35 atm. The static pressure in the vessel is measured by a commercial capacitance manometer at room temperature, while the swept pressure is monitored by a small Straty-Adams-type pressure transducer coupled to the vessel by a short length of capillary tubing.[6,7]

In a typical experimental run, the pressure vessel and cell are evacuated and flushed with helium gas at room temperature. The apparatus is then cooled to 4.2 K and helium is condensed until the vessel and cell are completely filled with pressurized liquid. The helium bath is then pumped until the desired temperature is reached. The infrared source is turned on and the radiation is chopped at a low frequency (≈ 10 Hz). Application of a

negative potential of 1500–3000 V to the field emission tips produces an electron current through the liquid helium of up to 1 μA. The current to the cell wall is monitored by a fast electrometer which is ac coupled to a lock-in detector. The lock-in detector derives its phase reference from the chopper, so its output is proportional to the ac component of the electron current at the chopper frequency.

EXPERIMENTAL RESULTS AND DISCUSSION

Experiment

Experimental traces can be taken by sweeping either the liquid helium pressure or the wavelength of the infrared radiation. When pressure is swept the wavelength and infrared power remain constant, but the field emission current (at constant voltage) varies with pressure. When the wavelength is swept, the pressure and field emission current remain constant, but the infrared power into the cell varies with wavelength. In this case, we can normalize the signal (lock-in output) to the photon flux in the cell by utilizing our HgCdTe detector to monitor the photon flux. A representative wavelength sweep normalized to the photon flux is shown in Fig. 1, where the 1s-1p transition line appears at 6.8 μm. The large linewidth of ≈ 1 μm arises from thermally excited vibrational modes of the bubble and is discussed below. By fitting a Gaussian line shape to the normalized data trace, we can readily determine the transition wavelength to within ± 0.1 μm ($\approx \pm 1\%$). The absolute pressure applied to the liquid helium is measured by a capacitance manometer to an accuracy of $\pm 0.1\%$. The temperature for the trace in Fig. 1 and for most of the work reported here is ≈ 1.25 K. The transition wavelength is independent of temperature in the small temperature interval where we took data.

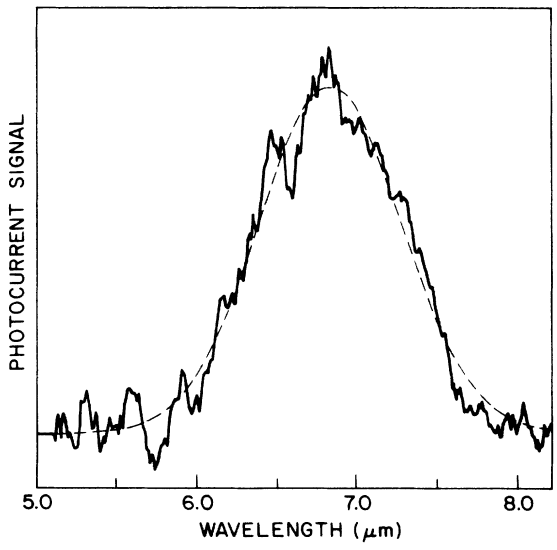

FIG. 1. The continuous line is a representative experimental trace displaying the electron bubble photocurrent signal (normalized to the photon flux) when the wavelength is swept at a constant pressure of 11.90 atm. The dashed line is a Gaussian fit to the trace. The 1s-1p transition is centered at a wavelength of 6.8 μm.

Results and discussion

The principal result of this work, the observed transition wavelengths and the corresponding pressures, are displayed in Fig. 2, where wavelengths have been converted to energies in eV. The calculated curves in Fig. 2 are discussed below.

At this point, it is instructive to review simple models of the electron bubble. In the simplest model the electron is viewed as residing in an infinitely deep spherical-square-well potential where the bubble radius is governed by the equilibrium between the inward pressures due to surface tension and pressure in the bulk liquid and the outward pressure due to localization of the electron. The total energy of the electron bubble can be written

$$E_T = E_e + \tfrac{4}{3}\pi R^3 P + 4\pi R^2 \sigma \ , \tag{1}$$

where E_e is the ground-state electronic energy given by $\hbar^2\pi^2/2m_e R^2$, the second term is the PV work done in forming the cavity, and the third term is the surface ener-

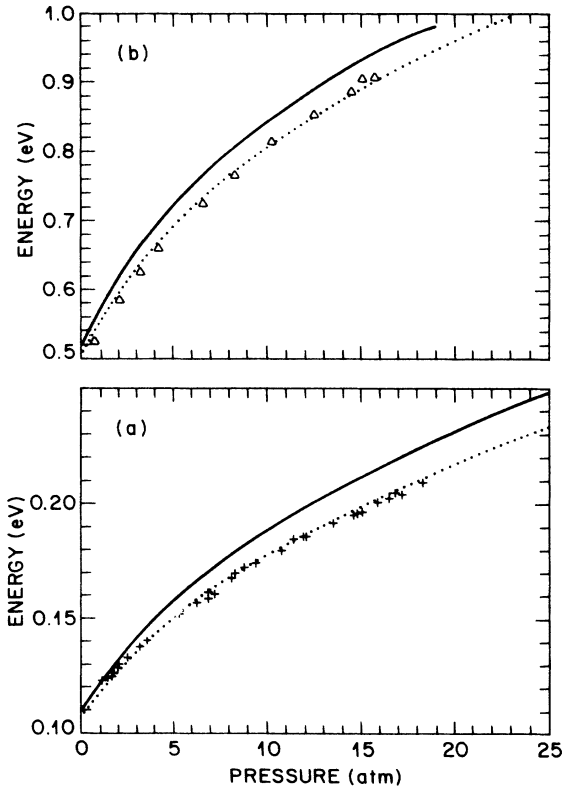

FIG. 2. Transition energies as a function of pressure for infrared transitions observed in the electron bubble photocurrent. The crosses in (a) are observed points for the 1s-1p transition. The open triangles in (b) are Zipfel's measured points for the 1s-2p transition (Ref. 4). The solid lines are from a calculation similar to that of Miyakawa and Dexter (Ref. 5) using a surface tension that increases with pressure. The dotted lines are calculated assuming the surface tension is independent of pressure.

gy. At equilibrium, the total energy is a minimum which yields the following relation between the radius and pressure:

$$P=\hbar^2\pi/4m_eR^5-2\sigma/R\ .$$

Taking $\sigma=0.341$ erg/cm^2, the radius becomes 19.36 Å at zero pressure and decreases to ≈ 12.5 Å at the solidification pressure (25 atm).[8-10] The eigenenergies for the infinitively deep spherical-square-well potential are derived in elementary quantum mechanics text books. The $1s$-$1p$ transition energy is $\Delta E_{1p}=0.105$ eV at $P=0$ and increases to $\Delta E_{1p}=0.232$ eV at 20 atm. Although pressure affects each term in Eq. (1), its primary effect on the transition energy is through the reduction in bubble radius, so even this simple model gives a reasonable estimate of the increase in ΔE.

Finite spherical-square-well potentials of depth V_0 are also treated in textbooks. The electronic eigenenergies take the form $E_{nl}=C_{nl}(V_0)/R^2$, where the $C_{nl}(V_0)$ are obtained from simple transcendental equations. The finite repulsive barrier allows the electronic wave functions to penetrate into the liquid helium which, for a fixed radius R, decreases each E_{nl} relative to their values for the infinitely deep potential well. The smaller electronic energy yields a smaller bubble radius when the total energy (1) is minimized. The equilibrium radius at $P=0$ varies as $\sigma^{-1/4}$. For a bubble of 18 Å radius, the surface tension exerts a pressure on the electron equivalent to $P\approx 4$ atm.

Several articles have presented calculated spectral properties of the electron bubble. Absorption, emission, and Raman scattering for pressures to 25 atm have been treated. In addition to the terms in (1), a small polarization energy term $-(\epsilon-1)e^2/2\epsilon R$ was included in some calculations. All of the terms in the total energy depend upon pressure either explicitly or implicitly through the dependence of V_0, σ, and ϵ on density, and this pressure dependence is incorporated in the calculations. Fowler and Dexter (FD) treated in detail the four bound states $1s$, $1p$, $2s$, and $2p$ in a spherical-square-well potential with $V_0(0)=1.02$ eV and $\sigma(0)=0.36$ erg/cm^2. They calculated the total energies of all four states as a function of bubble radius and displayed them in configuration coordinate diagrams. They deduced the equilibrium radius of each state and calculated the energies and oscillator strengths of the electric dipole allowed absorption and emission transitions.[11]

For the $1s$-$1p$ and $1s$-$2p$ absorption transitions MD (Ref. 5) extended these calculations with greater precision, included the polarization term, and employed a range of values for $V_0(0)$, the depth of the potential well at $P=0$. MD found that $V_0(P)$ increased about 20% over the pressure interval 0–25 atm for both an optical approximation and a Wigner-Seitz (WS) model calculation. The WS pressure variation of $V_0(P)$ was incorporated in their calculations and is used in our calculations. Their results for the $1s$-$1p$ and $1s$-$2p$ absorption transitions for $V_0(0)=1.02$ eV are displayed as solid curves in Figs. 2(a) and 2(b). Both MD and FD assumed that $\sigma(P)$ varied with P according to the theory of Amit and Gross.[12] Consequently, they took σ to vary from 0.36 at $P=0$ to 0.66 erg/cm^2 at $P=25$ atm. MD pointed out that reducing $V_0(0)$ to 0.948 eV improves the agreement with Zipfel's data in Fig. 2(b). However, we find that reducing $V_0(0)$ has very little effect on the calculated energies of the $1s$-$1p$ transition.

We find, in a calculation similar to MD's, that good agreement with experiment can be achieved for both transitions over the whole range of pressures studied if we retain $V_0(0)=1.02$ eV, but take $\sigma=0.341$ erg/cm^2 independent of pressure. The resulting transition energies are shown by the dotted curves in Figs. 2(a) and 2(b).

Fitting the spectroscopy data with a surface tension that is independent of pressure is unexpected. The pressure dependence of σ has never been measured, so several possible dependences have been considered. As mentioned above, the Amit and Gross theory predicts that σ will nearly double in the pressure interval 0–25 atm. Springett *et al.*[13] attempted to derive the pressure dependence of σ by combining the $R(P)$ measurements of Springett and Donnelly[14] with the predictions of their Wigner-Seitz model. They obtained an effective surface tension that increased about a factor of 3 in the pressure range 0–20 atm. In contrast, an earlier calculation by Hiroike *et al.*[15] found the surface tension in the bubble increasing approximately as the square of the helium density which amounts to about a 35% increase in σ at 20 atm.

These results indicate the need for more sophisticated calculations of the properties of electron bubbles. Such calculations need to incorporate the fact that the He density profile at the surface of the bubble is not abrupt, but rather varies smoothly from zero to the liquid density over a few angstroms. The modification of the effective surface tension due to the presence of the electron also needs to be treated.

Early variational calculations by Jortner *et al.*[16] and by Hiroike *et al.*[15] indicated that the helium-electron interface was nearly abrupt, so a square-well model should be a good approximation. More recently, Padmore and Cole, using a phenomenological model and variational calculations, found that the density profile at the surface of the bubble is only slightly "tighter" than at the free surface, and that the curvature contribution to the surface tension is very small ($\approx 1\%$).[17] They did not explicitly calculate the pressure dependence of the bubble properties.

Linewidth

Calculations by FD indicate that the absorption linewidth is primarily due to thermal excitation of the breathing and quadrupolar modes of oscillation of the electron bubble. The energy of the final state ($1p$ in this case) is a rapidly varying function of the bubble radius at the equilibrium radius of the ground $1s$ state. Quadrupolar distortions also strongly modulate ΔE_{1p}. These two effects combined lead to a predicted linewidth of ≈ 0.01 eV for the $1s$-$1p$ transition at 1.3 K. The observed linewidth (FWHM) increases smoothly from about 0.02 eV at low pressures to approximately 0.03 eV at the highest pressures.

Electron bubble radius

One of the fundamental parameters characterizing the electron bubble is its radius. Our spectroscopic measurements yield a direct determination of the bubble radius as it is defined in the spherical-square-well model where the transition energies depend only on R and V_0. Choosing a $\sigma(P)$ that fits the transition energies at all pressures is equivalent to assigning to $\sigma(P)$ the values that yield the correct radii to produce the observed splittings. The equilibrium bubble radius of the 1s ground state calculated using the parameters from the fit to the transition energies is displayed as the solid curve in Fig. 3. We find at zero pressure a radius of 17.2 Å which decreases to 11.1 Å at 25 atm. We estimate the cumulative errors in the radius determination to be about $\pm 1\%$. Relative radii deduced by Springett[18] from his measurements of the cross section for capture of bubbles on vortex lines are shown as open triangles in Fig. 3. He took the radius to be 15.96 Å at zero pressure which is the valued deduced by Parks and Donnelly[19] from Douglass's earlier trapping lifetime measurements.[20] Springett's data points lie consistently 1.2 Å below our curve. Ostermeier derived values of $R(P)$ from his accurate measurements of bubble mobility in the phonon-limited regime.[21] His results are displayed as the thin vertical bars in Fig. 3, and are in satisfactory agreement with ours over the pressure interval covered in our experiment. Poitrenaud and Williams obtained a precise value for the bubble effective mass in a resonance experiment on bubbles trapped beneath a free surface.[22] This measurement yielded a single data point, $R = 17.2 \pm 0.15$ Å at $P = 0$, in excellent agreement with our result. More recently, Ellis *et al.*[23] have derived bubble radii from effective mass measurements for pressures from 11 to 25 atm. Their results, also displayed in Fig. 3, lie consistently 1.5% above our solid curve. They estimate that their systematic errors are no larger than 0.7%. However, they also point out that incorporating a small quartic term in the energy-momentum relation for the electron bubble could reduce their effective masses by about 8% and the derived radii by 2%. This would bring their data into excellent agreement with our values for the bubble radius. Padmore and Cole,[17] in the variational calculation mentioned above, found a radius of 17.2 Å. They and Springett have emphasized that bubble radii deduced from different types of measurements may differ because they may not be defined the same way.

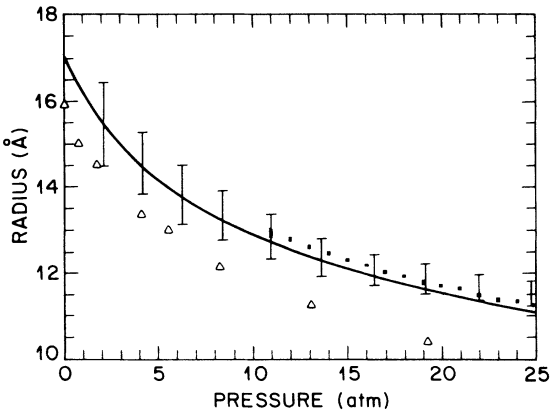

FIG. 3. The solid line shows the electron bubble radius as a function of pressure deduced from the spherical-square-well model of the bubble using the same well depth and surface tension as used to calculate the dotted lines in Fig. 2. The errors in this determination of the radius are estimated to be about 1% in the pressure interval 1–18 atm. The thin vertical bars are radii derived by Ostermeier from phonon-limited mobility measurements (Ref. 21). The wider vertical bars denote radii deduced by Ellis *et al.* from bubble acceleration measurements (Ref. 23). The open triangles are Springett's results from measurements of the bubble trapping cross section on vortex lines (Ref. 18).

Detection mechanism

In the Introduction, we mentioned that trapping of electron bubbles on vorticity appears to play a role in the photoconductivity detection mechanism. Northby[24] first suggested that photoionization of bubbles trapped on vorticity might account for the observed photoconductivity for excitation from the ground state to the continuum. Zipfel noted that at high pressure the photoconductivity signal for transitions between bound states became very temperature dependent and disappeared near the temperature and pressure where Springett found that vortices no longer trap electron bubbles. MD suggested that the photocurrent arises from a two-step process wherein the electron absorbs a photon and makes a transition to an excited state. Then the excited state bubble expands to a new, larger, equilibrium radius in a time of order $R/v_S \approx 10^{-11}$ s, where v_S is the velocity of sound in liquid helium. This sudden expansion raises the local temperature which thermally excites the electron bubble off of the vortex line so it contributes to the photocurrent. The characteristic time for this detection mechanism is quite small, probably $< 10^{-9}$ s. Experimentally, we find that the actual detection mechanism is slow: The response time is ≈ 0.1 s.

To gain insight into the actual mechanism that allows us to detect the transition as a photocurrent signal, we have studied how the 1s-1p transition signal disappears with increasing P or T. Several P, T, points where the signal disappeared are displayed as open triangular data points in Fig. 4. A single data point denotes the highest pressure where Zipfel observed the 1s-2p transition.[4]

In our experiments, which utilize field emission tips as electron sources, we expect the superfluid helium to contain a dense tangle of vorticity because electron velocities in the high field region near the tip exceed the critical velocity for vortex ring nucleation. McClintock has interpreted the peculiar temperature dependence of field emission currents in superfluid helium as arising from a tangle of vorticity.[25] The field emission current increases as T is lowered below the lambda point, passes through a maximum, and then falls by an order of magnitude or more before passing through a shallow minimum. The region where the field emission current is falling with decreasing T is the region where electron bubbles are spending an increasing fraction of their transit time trapped on vortici-

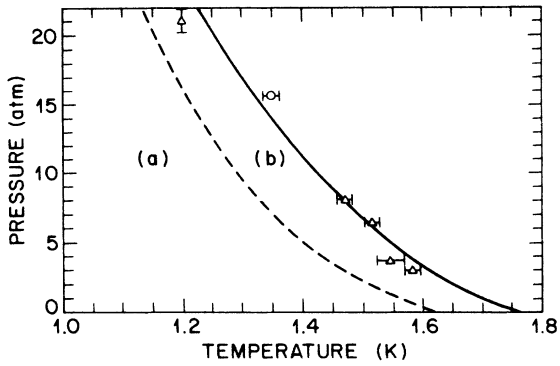

FIG. 4. Portion of the P-T plane showing correlation of loss of photocurrent signal and vanishing of the cross section for trapping of electron bubbles on vortex lines. Springett and Donnelly (Ref. 14) found the trapping cross section increased slowly with temperature in region (a), fell rapidly with increasing temperature in region (b), and extrapolated to zero at the solid line. The open triangles show the T,P values where the photocurrent signals for the $1s$-$1p$ transition vanished with increasing T. The open circle indicates where Zipfel's $1s$-$2p$ photocurrent signal vanished (Ref. 4).

ty. This is the region where the photoconductivity signal is observed.

Springett studied the trapping of electron bubbles on vortices as a function of P and T in a rotating cryostat. He found that at low temperatures bubbles are readily trapped on vortex lines by the Bernoulli force, but as the temperature is increased the electron bubbles can be thermally excited out of such traps and the trapping cross section drops rapidly to zero in a narrow temperature interval.[14,18] In Fig. 4 are displayed the three regions of the P-T plane where the trapping cross section is large and nearly T independent, where it drops rapidly with increasing temperature, and where it is negligible. Also shown in this figure are several data points denoting the temperatures and pressures where our observed $1s$-$1p$ transition signals vanished. These data pints were obtained by determining where the signal amplitude fell to zero on a recording of the signal amplitude versus T at fixed P and wavelength. A single data point denotes the highest pressure where Zipfel observed the $1s$-$2p$ transition.[4] All of these data points lie near the line in the P-T plane where the trapping cross section vanishes.

The photoconductivity signal for the $1s$-$1p$ transition weakens rapidly as P decreases below 3 atm, and is lost in the noise for $P < \approx 0.9$ atm. Zipfel and Sanders found that the $1s$-$2p$ photocurrent signal also decreased at low P and was not observable for $P \leq 0.7$ atm.[3] Its disappearance was attributed to the long wavelength cutoff of the glass Dewar walls which were in the optical path.[4] The disappearance at low P of the signals for the two transitions probably has a common cause. Two possible causes are discussed below.

The details of the photocurrent detection mechanism are not understood at this time. Clearly, the vanishing of our photocurrent signal at or near the pressures and temperatures where the cross section for the trapping of bubbles on vortices vanishes strongly supports the assumption that the photocurrent is associated with trapping of bubbles on vorticity. Any proposed detection mechanism must also yield an increase in current when the incident radiation is exciting $1s$-$1p$ transitions, it must operate only over a finite pressure interval, and it must account for the slow response mentioned above.

A possible explanation for the weakening of the signal at low P is to assume that the bubble distorts from its spherical shape. For electron bubbles trapped on vorticity, the anisotropy of the Bernoulli force should produce an elongation of the bubbles at low P. For a bubble centered on a vortex line, the $1/r$ velocity field of the vortex produces a Bernoulli pressure that is lower by several atmospheres near the poles of the bubble than it is at the equator. For small P, the Bernoilli pressure competes with the surface tension in determining the shape of the bubble. We estimate that the bubble may elongate by several percent. Due to this distortion the electronic ground state will no longer be a pure $1s$ state, but will contain an admixture of excited states. This mixing of states can modify the selection rules and oscillator strengths. The elongation of the bubble would remove the degeneracy of the m manifold of the $1p$ final state. This effect might appear as a broadening and then splitting of the $1s$-$1p$ transition. Distortion of the bubbles may make some otherwise forbidden transitions accessible to observation. We have looked for, but have not yet seen, such effects.

Another possible explanation for the vanishing of the $1s$-$1p$ signal at low pressures has recently been advanced by Elser.[26] He suggests that at pressures above ≈ 1 atm an electron bubble in the excited $1p$ state is unstable against a radiationless decay back to the ground state. In his proposed scenario, the p-state bubble elongates, removing the degeneracy of the m manifold with the $m=0$ state lying lowest in energy. The elongation continues while the "waist" of the hour-glass shaped bubble tends to pinch off. The electron ultimately settles into the cavity on one side of the waist leaving the cavity on the other side to collapse with the emission of phonons (heat). It is the released heat that drives the photocurrent. At pressures below ≈ 1 atm the p-state bubble is sufficiently stable to decay radiatively and not release enough heat to be detected in our photocurrent measurement.

Finally, we should mention that, using the cell containing the HgCdTe detector, we have looked for, but have not seen, a signal due to direct absorption of the infrared radiation. MD calculated the $1s$-$1p$ absorption cross section to be about 2×10^{-15} cm^2. Taken with our electron densities ($\approx 10^{-9}$ cm^3) and optical path length (≈ 10 cm), the fractional absorption of the infrared radiation incident on the detector is expected to be about $1{:}10^5$, which is too small for us to detect. It might be observable at lower temperatures where the linewidths are smaller.

CONCLUSIONS

We have employed a simple photocurrent measurement to observe for the first time the $1s$-$1p$ transition in

the electron bubble in liquid helium. This observation confirms the Miyakawa and Dexter suggestion that Zipfel observed the $1s$-$2p$ transition. The spherical-square-well model of the electron bubble accounts well for the data if the effective surface tension is taken to be independent of the applied pressure. The equilibrium bubble radii derived from this experiment are in satisfactory agreement with values deduced by Ellis *et al.* from acceleration measurements and with values deduced by Ostermeier from mobility measurements. Our radii display the same pressure dependence as was determined by Springett from the trapping lifetime of bubbles on vortex lines. The locus of points in the P-T plane where the signals vanish with increasing pressure indicates that the photoconductivity detection mechanism involves trapping of electron bubbles on vorticity.

ACKNOWLEDGMENTS

We gratefully acknowledge the guidance on optical matters provided by D. Rapkine, J. Orenstein, and G. Thomas and their loans of equipment that made this work possible. We have benefited from numerous stimulating discussions with Veit Elser.

[1]For comprehensive reviews of electrons in helium, see A. L. Fetter, in *The Physics of Liquid and Solid Helium*, Part I, edited by K. H. Bennemann and J. B. Ketterson (Wiley, New York, 1974), Chap. 3; K. W. Schwarz, in *Advances in Chemical Physics XXXIII*, edited by L. Prigogine and S. A. Rice (Wiley, New York, 1975); p. 1; and V. B. Shikin, Usp. Fiz. Nauk **121**, 457 (1977) [Sov. Phys. Usp. **20**, 226 (1977)].

[2]J. A. Northby and T. M. Sanders, Phys. Rev. Lett. **18**, 1184 (1967).

[3]C. Zipfel and T. M. Sanders, Jr., in *Proceedings of the Eleventh International Conference on Low Temperature Physics*, edited by J. F. Allen, D. M. Finlayson, and D. M. McCall (University of St. Andrews, Scotland, 1968), Vol. I, p. 296.

[4]C. L. Zipfel, Ph.D. thesis, University of Michigan, 1969 (unpublished).

[5]T. Miyakawa and D. L. Dexter, Phys. Rev. A **1**, 513 (1970).

[6]G. C. Straty and E. D. Adams, Rev. Sci. Instrum. **40**, 1393 (1969).

[7]I am indebted to D. S. Greywall for the loan of a pressure transducer which was described in D. S. Greywall and P. A. Busch, J. Low Temp. Phys. **46**, 451 (1982).

[8]For the $P=0$ values of V_0 and σ we take 1.02 eV and 0.341 erg/cm^2 at $T=1.25$ K the measured values reported in Refs. 9 and 10, respectively.

[9]M. A. Woolf and G. W. Rayfield, Phys. Rev. Lett. **15**, 235 (1965).

[10]M. Iino, M. Suzuki, and A. J. Ikushima, J. Low Temp. Phys. **61**, 155 (1985).

[11]W. B. Fowler and D. L. Dexter, Phys. Rev. **176**, 337 (1968).

[12]D. Amit and E. P. Gross, Phys. Rev. **145**, 130 (1966).

[13]B. E. Springett, M. H. Cohen, and J. Jortner, Phys. Rev. **159**, 183 (1967).

[14]B. E. Springett and R. J. Donnelly, Phys. Rev. Lett. **17**, 364 (1966).

[15]K. Hiroike, N. R. Kestner, S. A. Rice, and J. Jortner, J. Chem. Phys. **43**, 2625 (1965).

[16]J. Jortner, N. R. Kestner, S. A. Rice, and M. H. Cohen, J. Chem. Phys. **43**, 2614 (1965).

[17]T. C. Padmore and M. W. Cole, Phys. Rev. A **9**, 802 (1974).

[18]B. E. Springett, Phys. Rev. **155**, 139 (1967).

[19]P. E. Parks and R. J. Donnelly, Phys. Rev. Lett. **16**, 45 (1966).

[20]R. L. Douglass, Phys. Rev. Lett. **13**, 791 (1964); Phys. Rev. **141**, 585 (1965).

[21]R. M. Ostermeier, Phys. Rev. A **8**, 514 (1973).

[22]J. Poitrenaud and F. I. B. Williams, Phys. Rev. Lett. **29**, 1230 (1972); **32**, 1213(E) (1974).

[23]T. Ellis, P. V. E. McClintock, and R. M. Bowley, J. Phys. C **16**, L485 (1983).

[24]J. A. Northby, Ph.D. thesis, University of Minnesota, 1966 (unpublished).

[25]P. V. E. McClintock, J. Phys. C **6**, L186 (1973).

[26]Veit Elser (private communication); (unpublished).